

Origin of polar nanoregions and relaxor properties of ferroelectrics

Victor Polinger¹ and Isaac B. Bersuker²

¹*Department of Chemistry, University of Washington, Box 351700, Seattle, Washington 98195-1700, USA*

²*Institute for Theoretical Chemistry, The University of Texas at Austin, Austin, Texas 78712-1229, USA*

 (Received 19 August 2018; revised manuscript received 18 October 2018; published 4 December 2018)

In spite of more than 60 years of research, hundreds of publications, and dramatic influence on properties, the driving force of the formation of the polar nanoregion (PNR) in the paraelectric phase of perovskite ferroelectrics and consequent relaxor properties remains uncertain. We show that these peculiar features follow directly from the vibronic, pseudo-Jahn-Teller (PJT) theory of ferroelectricity. Due to the higher disorder (and entropy) in the paraelectric phase (created by the local PJT dynamics), as compared with the polarized phase (where the PJT dynamics is partially quenched), a small PNR of the latter with n unit cells is formed in a dipole-alignment self-assembly process. It emerges encapsulated by a border layer with intermedium ordering that produces “surface tension” and limits its size. The thermodynamic equilibrium between the PNR and the bulk cubic phase at temperatures T_n , well above the phase transition T_C , is reached by compensation of the excessive entropy contribution $T_n \Delta S$ with ordering energy and the work against this surface tension. The calculations based on the vibronic theory, including the PJT induced local dipolar dynamics and intercell interactions, yield the size of PNR as a function of the temperature increments $T_n - T_C$ and some crystal parameters. In accordance with experimental data, the size of the emerging PNR decreases with temperature, $n \sim (T_n - T_C)^{-3}$, becoming undetectable at the Burns temperature T_B . At temperatures T_f , nearer to the phase transition, the sizes of PNRs grow rapidly, and their interaction leads to the formation of the nonergodic (glasslike) phase.

DOI: [10.1103/PhysRevB.98.214102](https://doi.org/10.1103/PhysRevB.98.214102)

I. INTRODUCTION

Polar nanoregions (PNRs) or “polarized microdomains” in the nonpolarized, paraelectric phases are observed practically in all perovskite ferroelectrics. They are presently well studied experimentally, as they strongly influence all the properties of these systems (see [1–3], and references therein). The basic facts are as follows: In the paraelectric phases of ferroelectrics, above the Curie temperature T_C , where the bulk crystal is cubic and no polarization is expected, small islands (nanoregions) with a limited number n of unit cells are spontaneously formed, their size decreasing with increasing temperature $T_n - T_C$. Above the temperature T_B , called the Burns temperature, the PNRs disappear, and the crystal becomes regular and paraelectric. In addition, PNRs disappear under external, sufficiently strong electric fields that make the crystal regularly polarized. At this stage the paraelectric phase remains ergodic. With cooling, PNRs grow in size [4], and at a temperature T_f (closer to T_C , $T_C < T_f < T_B$) relaxor properties change again to a nonergodic, glasslike state [5–8], which then, at a somewhat smeared (diffuse) temperature around T_C , undergo the phase transition to the tetragonal polarized state. Again, distinguished from dipole glasses, this nonergodic state of the crystal can be irreversibly transformed into a regular polarized state by strong enough external electric fields. These are *relaxor ferroelectrics*.

There are no conclusive explanations of the origin of PNR and consequent relaxor properties, although several suggestions were discussed in the literature (see [1–3,9–12]). The majority of them, referring to the most studied mixed perovskites, rely (in different forms) on the assumption of

basic structural disorder or “random fields.” However, random fields or other “raisins-in-the-cake” crystal imperfections do not explain the origin of temperature-dependent size effects, in particular, the disappearance of PNR above T_B , or under polarizing electric fields. Notably, PNRs are present also in pure ferroelectric perovskites ABO_3 crystals [13–16]. Again, the considerations above do not answer the question why PNRs occur in ferroelectrics only, and do not show up in very similar nonferroelectric crystals with structural phase transitions.

So far, attempts to explain the origin of PNRs are based on the so-called “displacive” theories of ferroelectricity, in which the basic idea is that the ferroelectric distortion of the crystal occurs as a result of the compensation of the local repulsions (resisting dipolar displacements) by long-range dipole-dipole attractions. The theories based on these classical ideas are in essence phenomenological: They do not explain the origin and properties of ferroelectrics based on their chemical composition and structure, and they fail to explain the origin of dozens of experimental observations of peculiar properties of perovskite ferroelectrics (see below). Obviously, due to their microscopic size, several nanometers, the PNRs and their polarization are of local origin; long-range theories cannot explain nucleation of local polarization from zero to the nanosize and their further growth with cooling.

On the other hand, the vibronic (pseudo-Jahn-Teller) theory provides for a direct microscopic description of the origin of ferroelectricity in perovskite-type crystals based on first principles (see [17–23] including the review [18], and references therein). Starting with the high-symmetry (cubic) configuration, the vibronic coupling, by mixing the ground

state with appropriate excited electronic states, under limiting conditions makes this configuration unstable with respect to polar distortions. In its turn, this triggers the spontaneous polarization of the crystal, realized by intercell interactions. It is important that the pseudo-Jahn-Teller effect (PJTE) is induced by the off-diagonal matrix elements of the Hamiltonian derivatives, which are significantly nonzero for near-neighbor atomic wave functions' overlaps only [see below, Eq. (2)]. Therefore the PJTE in crystals is of *local origin* [17–20,24]; it does not contribute to long-range interactions. For this reason, the vibronic PJTE theory of ferroelectricity starts with the operator of vibronic coupling applied to the local ferroelectric centers (e.g., the B center in ABO_3 perovskites; similar treatment is possible for active A centers), but includes the influence of the whole crystal via its electronic and phonon bands. This treatment has been realized by means of the Green's functions approach [20]. Also, exclusively, the vibronic theory revealed the role of spin in the spontaneous polarization [19] and the origin of multiferroics in function of the electronic d^n configuration of the B ion, as well as the origin of giant perturbation effects [22,23], including giant flexoelectricity, permittivity, and electrostriction (for the flexoelectricity effect see, e.g., [25]).

One of the important results of the vibronic theory is the order-disorder nature of the ferroelectric phase transitions. Predicted in 1966 [17], the picture of the (induced by the PJTE) four phases in ferroelectric perovskites, one ordered, two partially disordered, and one fully disordered (paraelectric), and the order-disorder phase transition between them, was first observed experimentally in 1968 in $BaTiO_3$ and $KNbO_3$ by means of diffuse x-ray scattering [26]. In the years that followed, a huge variety of direct and indirect experimental observations (some of which presented unsurmountable difficulties for the displacive theories to explain their origin) were shown to follow directly from the vibronic (PJTE) theory of ferroelectricity (see the review paper [18]). Among them, we emphasize here the instant trigonal displacement of the B ion of the ferroelectric ABO_3 perovskite, notably $BaTiO_3$, *in all its four phases*, ferroelectric and paraelectric, *in strong disagreement* with displacive theories, in which the metal off-center displacement occurs as a result of the phase transition to the polarized phase. This fundamental property of perovskite ferroelectrics is confirmed by a variety of experimental data, actually by any observation that includes the B displacement, notably the extended x-ray absorption fine structure experiments [27] (see also [18,28–31]). Not only is the B ion displaced along the [111]-type direction in the paraelectric phase, where the averaged symmetry is cubic, but it is as well displaced in this trigonal direction in the tetragonal phase, where the crystal symmetry and the macroscopic polarization are tetragonal [29]. The most striking example is the off-center displacement of the Ti atom in barium titanate observed in the paraelectric phase way above the Curie temperature of the tetragonal-to-cubic phase transition. As accurate measurements indicate [27], the Ti ion remains displaced closely along [111] directions *throughout all the four $BaTiO_3$ phases*, and the magnitude of the off-center displacement decreases monotonically by only 13% when heating from 35 to 590 K, showing *no steps at the phase transitions*.

In this paper we consider nucleation and temperature-dependent growth of nanosize polarization islands (PNRs) in a cubic perovskite single crystal in its high-temperature paraelectric phase. PNRs are shown to occur as an intrinsic and physically quite transparent property of perovskite ferroelectrics, a natural consequence of the disorder produced by the local PJTE. In Sec. II we begin with a *very brief* description of the PJT approach and some of the results of this theory [17–20] employed in this paper. In Sec. III the formation of PNRs is shown to emerge as a result of a self-assembly process of alignment of the local PJT induced dipolar distortions, leading to relaxor properties. In Sec. IV and in the Conclusions section, a more detailed discussion of the results in their comparison with experimental data and with general theories of this kind, like “classical nucleation theory,” are given.

II. DYNAMIC POLAR DISTORTIONS IN THE PARAELECTRIC PHASE

As mentioned above, the vibronic coupling is of local origin; it does not include long-range interactions. Therefore, in perovskite crystals ABO_3 , in a reasonable approximation, the local polar instability can be treated as off-center displacement of the B ion from its on-center position in the elementary cell (Fig. 1). If the atom A is active as well, or even more than the B ion, the problem can be handled in a similar way. As a rule, B^{4+} is an ion of a transition metal, its electronic properties being defined by its relatively small-radius d electrons coupled to the near-neighbor atoms only. In other words, in dielectric perovskite crystals, the local PJT instability of the B^{4+} ion can be revealed by considering the closed-shell configuration of the octahedral cluster $[BO_6]^{8-}$. In the adiabatic approximation, the ground electronic state of this cluster is a function of polar coordinates, denoted by X, Y, Z , which are components of the local T_{1u} mode. They describe off-center displacement $\mathbf{R}(X, Y, Z)$ of B^{4+}

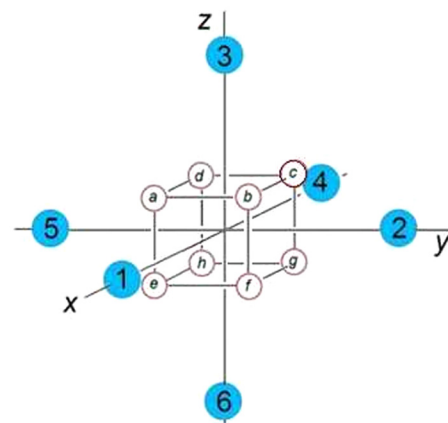


FIG. 1. The octahedral fragment of the perovskite crystal structure ABO_3 with the transition-metal atom B at the center (red) and six oxygen atoms at the apexes of the octahedron (numbered, blue). The letters a – h denote the eight equivalent off-center positions, induced by the PJTE, of the atom B in the eight wells of the APES. (Reprinted with permission from Ref. [20]. Copyright 2015 Elsevier Publishing.)

toward oxygen atoms and a counterphase displacement of the near-neighbor oxygen octahedron. The vibronic PJT coupling between the ground electronic state [the highest occupied molecular orbitals, (HOMOs), formed by mostly oxygen $2p$ electrons] with the excited state [the lowest unoccupied molecular orbitals (LUMOs), mostly the transition-metal $3d$ electrons] via the nuclear T_{1u} displacements determines the adiabatic potential energy surface (APES), $U(X, Y, Z)$. The problem for the high-symmetry $[BO_6]^{8-}$ cluster with its closed-shell electronic structure, reduced to a matrix 9×9 , yields its APES in the analytic form, already obtained in the previous paper about the PJTE theory [17] (see also [18,20]) as follows:

$$U(\mathbf{R}) = \frac{1}{2}K_0R^2 - 2[\sqrt{\Delta^2 + 2F^2(R^2 - X^2)} + \sqrt{\Delta^2 + 2F^2(R^2 - Y^2)} + \sqrt{\Delta^2 + 2F^2(R^2 - Z^2)}], \quad (1)$$

where $R^2 = X^2 + Y^2 + Z^2$, 2Δ is the (band adapted [20]) energy gap between the PJT active ground and excited electronic states, $\frac{1}{2}K_0R$ [2] is the added elastic energy with respect to these displacements, K_0 is the respective primary (nonvibronic) force constant, characterizing the crystal stiffness without the vibronic coupling (presented as a crystalline multimode sum with the expansion of \mathbf{R} over the corresponding crystal vibrations [20]), and F is the vibronic coupling constant; for $BaTiO_3$,

$$F = \langle 2p_y(O) | \left(\frac{\partial H}{\partial X} \right)_0 | 3d_{xy}(Ti) \rangle. \quad (2)$$

Here H is the electron-vibrational Hamiltonian of the cluster $[TiO_6]^{8-}$, $|2p_y(O)\rangle$ is the atomic $2p_y$ orbital of oxygen in the mentioned above HOMO, $|3d_{xy}(Ti)\rangle$ is the $3d_{xy}$ atomic orbital of the titanium ion in the LUMO, and $(\partial H/\partial X)_0$ is the corresponding component of the operator of vibronic coupling. Shown in Fig. 2 projected on a sphere, the APES of Eq. (1) is *very special* for transition-metal perovskites. Under

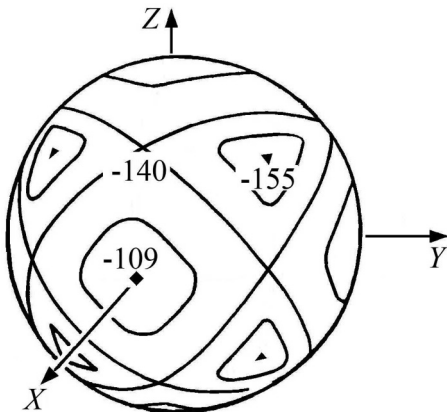


FIG. 2. Contour map of the ground-state APES $U(X, Y, Z)$ of the octahedral cluster $[TiO_6]^{8-}$ after Eq. (1). Points of the radius- R sphere correspond to actual displacements of Ti^{4+} ($R \approx 0.24 \text{ \AA}$). Equipotential level curves are labeled with the corresponding values of $U(X, Y, Z)$ in meV, same as in Table I, measured from the zero value at $R = 0$. Solid triangles represent trigonal (rhombohedral) minima, the black square is a tetragonal extremum, and orthorhombic saddle points are at the level curve's intersections.

TABLE I. Numeric estimates of the PJTE parameters of the APES, including the Ti ion displacement along Q and PJTE stabilization energies E_{JT} at the minima and saddle points [20].

K_0	6.82 meV/\AA^2
F	0.42 meV/\AA
$ X = Y = Z $	0.14 \AA
$ X = Y = q_0, Z = 0$	$q_0 = 0.16 \text{ \AA}$
$U(0, 0, 0)$	0 meV
$E_{JT}[100]$	109 meV
$E_{JT}[110]$	140 meV
$E_{JT}[111]$	155 meV

the condition

$$\Delta < \frac{8F^2}{K_0}, \quad (3)$$

$U(\mathbf{R})$ has a maximum with the B ion in the center, eight equivalent minima situated along the eight trigonal directions toward the cubic vertices; 12 equivalent saddle points along the six second-order symmetry axes C_2 (in two directions from the center), each of them forming an energy barrier between two near-neighbor equivalent minima; and six equivalent, higher-in-energy saddle points along the three tetragonal C_4 axes (in two directions), each of them forming a higher barrier between the groups of four near-neighbor equivalent minima. Numerical values of the parameters of this APES for $BaTiO_3$, obtained involving empirical data on the forbidden gap $2\Delta = 2.8 \text{ eV}$ and DFT calculated $\hbar\omega = 23.9 \text{ meV}$, are shown in Table I.

With the APES (1), the picture of all four phases of $BaTiO_3$ and the order-disorder phase transitions between them, as well as the variety of specific properties of such perovskite ferroelectrics, gets a full explanation, the main predictions of the theory being confirmed after their publication (for references see [18,20]). In barium titanate the totally symmetric configuration at $X = Y = Z = 0$ is very high in energy, $\Delta U = E_{JT}[100] \approx 109 \text{ meV} = 1270 \text{ K}$, as compared with the Curie temperature $T_C \approx 360 \text{ K}$. This means that the paraelectric phase is reached not by population of the states at the maximum of the free energy, but by the averaging of the arbitrary oriented dipoles via their overcoming the much lower orthorhombic and tetragonal barriers. A more rigorous theoretical treatment of this problem yielding a reasonably good agreement with the experimental values of the Curie temperatures was obtained recently in the mean field approximation [21]. The basic parameter of the theory is the averaged polarization per unit cell $[BO_3]^{8-}$, $\bar{p} = \bar{p}_{\text{nuc}} + \bar{p}_{\text{el}}$, induced by the PJTE. Here \bar{p}_{nuc} is the average ionic contribution, and \bar{p}_{el} is the average electronic dipole moment that emerges due to the polarization of the electronic shell. Because of the vibronic coupling these two contributions are proportional to one another, $\bar{p}_{\text{el}} = \text{const.} \cdot \bar{p}_{\text{nuc}}$. Therefore $\bar{p} = \bar{p}_{\text{nuc}} + \bar{p}_{\text{el}} = \bar{p}_{\text{nuc}} + \text{const.} \cdot \bar{p}_{\text{nuc}} = (1 + \text{const.})\bar{p}_{\text{nuc}}$ [21]. The factor $1 + \text{const.}$ can be rationalized by substituting the real charge of the central ion by the so-called Born effective charge Z_B . The localization of the nuclear motion at the extremum points of the APES produces an average dipole moment $\bar{p} = eZ_B\bar{R}$, where $R = |\mathbf{R}| = \sqrt{X^2 + Y^2 + Z^2}$ is the PJTE displacement of the ion B from the center of the octahedron.

By comparison, we can see that these R values are almost the same at different extrema points of the APES, $U(X, Y, Z)$ of Eq. (1). Indeed, according to the data in Table I, in the trigonal minima $R[111] \approx (0.14 \text{ \AA})\sqrt{3} \approx 0.24 \text{ \AA}$, while at the orthorhombic points $R[110] \approx (0.16 \text{ \AA})\sqrt{2} \approx 0.23 \text{ \AA}$, and along the shortest way between two near-neighbor trigonal minima via the orthorhombic saddle points (see Fig. 1) the potential energy does not change significantly: $E_{JT}[111] \approx 155 \text{ meV}$, and $E_{JT}[110] \approx 140 \text{ meV}$. This means that the bottom of the APES for BaTiO₃ Eq. (1) is a warped through, and the warping is relatively small. In other words, the motion of the Ti ion in the cluster $[BO_6]^{8-}$ can be reduced to reorientations of the electrical dipole moment \mathbf{p} via tunneling or hopping, its absolute value remaining unchanged: $|\mathbf{p}| = \bar{p} = eZ_B \bar{R}$. In this respect, the ferroelectric properties of cubic perovskites in the paraelectric phase are similar to polar liquids, or to systems with easily reorienting magnetic moments.

It follows that in a reasonable approximation such perovskite ferroelectrics can be treated as an electric analog of the Heisenberg model for coupled dipoles: [21,32],

$$H = -\frac{1}{2} \sum_{\mathbf{m} \neq \mathbf{n}} J(\mathbf{m} - \mathbf{n}) \mathbf{p}_{\mathbf{m}} \cdot \mathbf{p}_{\mathbf{n}}, \quad (4)$$

where $\mathbf{p}_{\mathbf{m}}$ is the dipole moment of the center \mathbf{m} , and $J(\mathbf{k})$ is the parameter of the intercenter interaction.

In brief, the picture of the ferroelectric phase transitions looks as follows [17,18,21]. Both the local dynamic off-center displacement and the mean field of the environment are interdependent in a self-consistent way. Lowering the temperature results in several consecutive phase transitions. In what follows we consider two phases: the high-temperature cubic paraelectric phase and tetragonal ferroelectric phase that occurs below the Curie temperature T_C . At $T > T_C$, the mean field $\mathbf{E} = 0$, the eight possible off-center positions of the ion B are equivalent (see the red line in Fig. 3). The local dipole moments are (macroscopically) averaged over all eight trigonal wells, along all eight crystal directions [Fig. 4(b)] the average dipole moment and hence the polarization equal zero, and the crystal is in the *completely disordered* paraelectric phase.

At lower temperatures, $T < T_C$, a nonzero mean field occurs [21], $\mathbf{E} \neq 0$, and the different dipole orientations

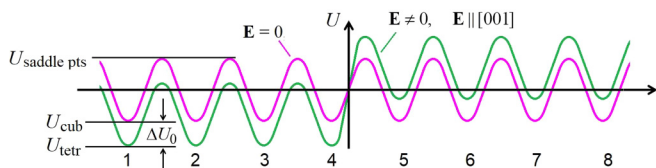


FIG. 3. Schematic cross section of the APES $U(X, Y, Z)$ along the path of steepest descent from the orthorhombic saddle points to the trigonal minima. At $T > T_C$, in the cubic phase the mean field equals zero, $E = 0$, and all the eight trigonal minima have the same depth (rose curve). At $T < T_C$ (green curve) the mean field is oriented along one of the tetragonal axes (here along $[001]$) lowering the energy of four minima 1, 2, 3, and 4 ($a-d$ in Fig. 1) and elevating the energy of the other four minima. The numeration of the minima is the same as in Fig. 4.

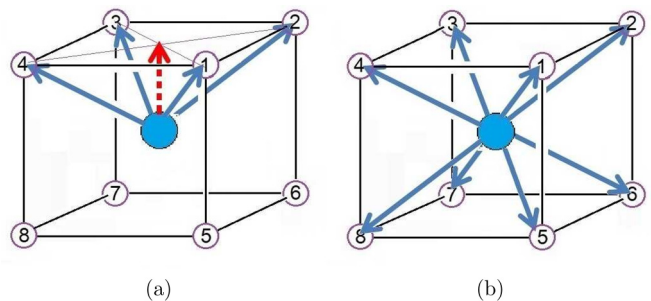


FIG. 4. Orientation of the local dipole moments in the eight minima of the cluster $[BO_6]^{8-}$ (the oxygens are not shown): (a) In the tetragonal phase at $T < T_C$, the dipole moments at different centers occupy (with equal probability) one of the four minima around the same axis C_4 , resulting in an average nonzero polarization in the direction of this axis (shown by red dashed arrow). (b) In the paraelectric phase, at $T > T_C$, all eight trigonal minima are equally populated; the averaged dipole moment and the polarization equal zero.

become nonequivalent due to the mean field of the environment induced by the instant off-center positions of the B ions in the near-neighbor cells. In this phase the mean field \mathbf{E} is oriented along one of the fourth-order axes, say, $[001]$ [Fig. 4(a)].

It lowers the energies of four adjusted minima, simultaneously elevating the energies of the remaining four (see the green curve in Fig. 3). Accordingly, the temperature controlled population of the first four minima increases, while decreasing in the other four, the majority of dipoles thus becoming oriented along the corresponding tetragonal axis [Fig. 4(a)]. Driven to the minimum of free energy, the crystal becomes *ordered* along the z axis, but remains *disordered* along its two other symmetry axes x and y . Macroscopically, this type of ordering is seen as the tetragonal phase. Still, lowered by the mean field, these four potential wells are separated from the other four by tetragonal potential barriers that are higher in energy.

III. FORMATION OF POLAR NANOREGIONS AND THEIR “SURFACE TENSION”

As mentioned above, tetragonal PNRs occur in the cubic paraelectric phase of the ferroelectric crystal (Fig. 5) at temperatures well above the Curie temperature, $T > T_C$, where the condition of thermodynamic equilibrium for the Helmholtz free energy, $\Phi_{\text{cub}} = \Phi_{\text{tetr}}$, does not hold. They decrease in size with increasing temperature and disappear above the Burns temperature T_B . The vibronic (PJTE) origin of perovskite ferroelectricity and order-disorder phase transitions between its different phases, briefly outlined above, reveals directly the driving force in the formation of PNRs and its main features. Like in all the other applications (e. g., the origin of giant flexoelectricity, [22] permittivity [22,23], and electrostriction [22]), the point is in the local dynamics of the dipolar distortions at the B centers, which are fully disordered (uncorrelated) in the paraelectric phase and partially ordered (correlated) in the ferroelectric phases. In bulk, at temperatures above T_C , the Helmholtz free energy of the cubic phase Φ_{cub} is lower than its value in the tetragonal

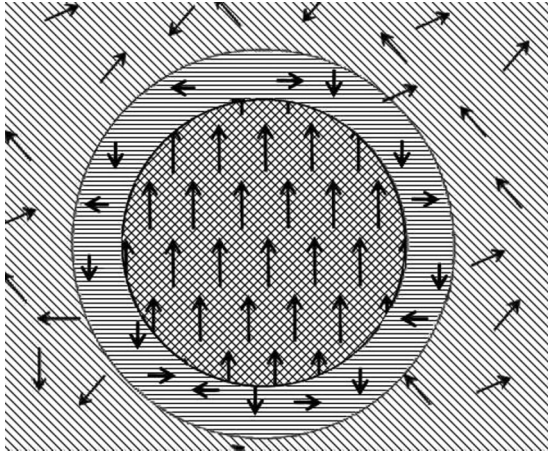


FIG. 5. Polarized nanoregion of spherical form (central circle) with the border layer (outlined) inside the bulk cubic perovskite at temperatures T above the Curie temperature T_C , but below the Burns temperature T_B ; $T_C < T < T_B$. Arrows indicate the direction of the local averaged dipole moments, which are tetragonally ordered inside the PNR and fully disordered in the cubic phase. For the role of the PNR surface layer, see the text.

phase Φ_{tet} . Accordingly, as $\Phi = U - TS$, in the temperature interval $T_C < T < T_B$ we have

$$T(S_{\text{cub}} - S_{\text{tet}}) > U_{\text{cub}} - U_{\text{tet}}. \quad (5)$$

Here U_{cub} and S_{cub} are, respectively, the potential energy and entropy per unit cell in the high-temperature paraelectric phase, whereas U_{tet} and S_{tet} are their respective values in the tetragonal phase. In other words, in bulk, lowering potential energy from (average) cubic to (average) tetragonal does not provide enough energy gain, $\Delta U = U_{\text{cub}} - U_{\text{tet}}$, to compensate the corresponding entropy loss $T(S_{\text{cub}} - S_{\text{tet}})$ at $T > T_C$.

Yet, local polarized isles (polar nanoregions, PNRs, Fig. 5) with a limited, relatively small number n of centers may still be formed. As shown below, at $T_n > T_C$ the inequality (5) is compensated by the transformation of a part of the tetragonal potential energy ΔU_{tet} of the PNRs into work of formation of its surface W_n . Indeed, the gain of energy in the formation of the n -center PNR $\Delta U_n = U_n^{(\text{cub})} - U_n^{(\text{tet})}$ consists of two contributions: $\Delta U_n^{(\text{in})}$, the energy of the internal centers, i.e., the energy of the ordering the dipoles inside the PNRs [all oriented, in average, along the polarization direction, Fig. 4(a)], and $\Delta U_n^{(\text{surf})}$, the energy of the centers in the surface layer, that are influenced by the neighbor disordered centers of the cubic phase (Fig. 5).

Consider $\Delta U_n^{(\text{in})}$ in the mean field approximation, briefly outlined above. The energy of the ordered (correlated) dipoles can be accounted for by the Hamiltonian (4), with $\mathbf{p}_m = \langle \mathbf{p}_m \rangle + \Delta \mathbf{p}_m$, where $\langle \mathbf{p}_m \rangle$ is the average dipole moment of the center \mathbf{m} , and $\Delta \mathbf{p}_m = \mathbf{p}_m - \langle \mathbf{p}_m \rangle$ is its related fluctuation. Substituting $\Delta \mathbf{p}_m = \mathbf{p}_m - \langle \mathbf{p}_m \rangle$, and keeping only terms linear in $\Delta \mathbf{p}_m$, we come to the additive Hamiltonian $H = \sum_m H_m$, where

$$H_m = -\mathbf{p}_m \cdot \sum_{n \neq m} J(\mathbf{m} - \mathbf{n}) \langle \mathbf{p}_n \rangle = -\mathbf{p}_m \cdot \mathbf{E}_m. \quad (6)$$

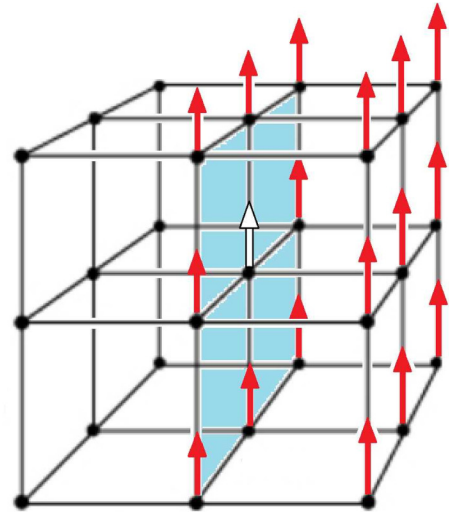


FIG. 6. Mean field E directions (shown by arrows) for the inner and border centers of the PNR. Within the tetragonally ordered bulk to the right of the border surface (shown in blue) each center is positioned in the mean field of six near-neighbor centers with the same direction of the field, whereas for each center on the border (e.g., the one in the center of the fragment shown by white arrow) only five near-neighbor centers contribute to its mean field.

Here $\mathbf{E}_m = \sum_{n \neq m} J(\mathbf{m} - \mathbf{n}) \langle \mathbf{p}_n \rangle$ is the vector of the mean field at the center \mathbf{m} . In the tetragonal phase all the dipoles are formed by the B^{4+} ions at the four minima 1, 2, 3, 4 of the APES [Fig. 4(a)], where they have the same average value $|\mathbf{p}| = \bar{p} = eZ_B \bar{R}$, and are directed at an acute angle of 54.7° with respect to the average field direction. Then from Eq. (6) we get the gain of energy per center by ordering as follows: $\Delta U_0^{(\text{in})} \approx E \bar{p} \cos(54.7^\circ) = \frac{E \bar{p}}{\sqrt{3}}$. Similarly, the dipoles in the remaining four trigonal minima 5, 6, 7, 8 are oriented along an obtuse angle of 125.3° with respect to the mean field, and their energy is elevated by the same amount (Fig. 3, the green line).

The parameter $J(\mathbf{m} - \mathbf{n})$ stands for the intercenter interaction. In the main part of the dipole-dipole interaction it descends rapidly with the intercenter distance, $J(\mathbf{m} - \mathbf{n}) \sim |\mathbf{m} - \mathbf{n}|^{-3}$. Therefore, approximately, for the internal centers the gain in energy from ordering in the PNRs is the same as in the bulk tetragonal phase. Per one center it is $\Delta U_0^{(\text{in})} = U_{\text{cub}} - U_{\text{tet}} = \Delta U_0$ [cf. Eq. (5)]. In $H = \sum_m H_m$ the sum is over the number of fully ordered centers in the PNRs, $n - n'$, where n' is the number of centers in the surface layer (in what follows, the surface layer is assumed to be about one lattice constant thick, but actually more centers may be affected). Accordingly, the energy gain in the formation of the PNR due to the tetragonal ordering is $\Delta U_n^{(\text{in})} = (n - n') \Delta U_0$.

The mean field for the n' centers of the surface layer is different from that in the bulk of the tetragonal PNR. Indeed, in the cubic perovskite crystal each dipolar B center has six near-neighbor B centers, all of which contribute to the mean field in the polarized phase, but only five of them contribute to the mean field acting upon the surface center (Fig. 6). The sixth near-neighbor center belongs to the fully disordered cubic phase where the mean field is zero. Therefore, for a

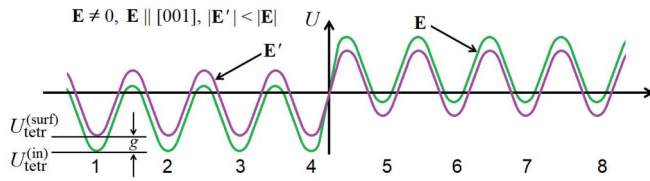


FIG. 7. For the centers on the surface of the PNR the tetragonal mean field ($E, E' || [001]$) is weaker, $|E'| < |E|$, and the lowest minima 1–4 on the APES (shown by purple curve) are shallower by g than the ones for the inside centers (green curve); cf. Fig. 3.

plane wall, the tetragonal mean field in the wall is weaker than inside the PNR, $E' \approx \frac{5}{6}E$ (in fact the wall is not planar, so the E' value may be lower). Accordingly, on the surface of the PNR trigonal wells of the APES are shallower than inside the PNR, $U_{\text{tetr}}^{(\text{surf})} < U_{\text{tetr}}^{(\text{in})}$, as shown in Fig. 7. Per one center, introducing $g = U_{\text{tetr}}^{(\text{surf})} - U_{\text{tetr}}^{(\text{in})}$, we get $\Delta U_0^{(\text{surf})} = U_{\text{cub}} - U_{\text{tetr}}^{(\text{surf})} = U_{\text{cub}} - U_{\text{tetr}}^{(\text{in})} - g = \Delta U_0^{(\text{in})} - g = \Delta U_0 - g$. For n' surface centers $\Delta U_n^{(\text{surf})} = n'(\Delta U_0 - g)$; hence

$$\begin{aligned} \Delta U_n &= \Delta U_n^{(\text{in})} + \Delta U_n^{(\text{surf})} = (n - n')\Delta U_0 + n'(\Delta U_0 - g) \\ &= n\Delta U_0 - n'g. \end{aligned} \quad (7)$$

The potential energy of the PNR is thus $U_n^{(\text{tetr})} = U_n^{(\text{cub})} - n\Delta U_0 + n'g$, or, by taking $U_n^{(\text{cub})} = 0$ as the energy read-off, we get

$$U_n^{(\text{tetr})} = -n\Delta U_0 + n'g. \quad (8)$$

To avoid misunderstanding, we emphasize here that, as it follows from the detailed consideration above, the border layer of the PNR separates two different phases, one paraelectric and the other one ferroelectric, coexisting in the same crystal at the same temperature, and as such, it is *essentially different* from domain walls.

Consider, for example, the PNR of spherical form (which seems to be dominant) with the radius r . In the cubic crystal with the unit cell dimension a , the number of centers in a spherical PNR equals the ratio of their volumes:

$$n = \frac{\text{Volume of the sphere}}{\text{Volume of one unit cell}} = \frac{\frac{4}{3}\pi r^3}{a^3} = \frac{4\pi}{3} \left(\frac{r}{a}\right)^3. \quad (9)$$

Hence,

$$\begin{aligned} \frac{r}{a} &= \sqrt[3]{\frac{3n}{4\pi}} = \sqrt[3]{\frac{3}{4\pi}} n^{1/3} \approx 0.62n^{1/3}, \quad \text{or} \\ r &= a \sqrt[3]{\frac{3}{4\pi}} n^{1/3} \approx 0.62an^{1/3}, \end{aligned} \quad (10)$$

while the number of cells on the surface equals

$$\begin{aligned} n' &= \frac{\frac{4}{3}\pi r^3 - \frac{4}{3}\pi(r-a)^3}{a^3} \approx 4\pi \left(\frac{r}{a}\right)^2 \\ &= \sqrt[3]{36\pi} n^{2/3} \approx 4.8n^{2/3}. \end{aligned} \quad (11)$$

Substituting Eqs. (9) and (11) into (8), we get

$$\begin{aligned} U_n^{(\text{tetr})} &= -\frac{4\pi}{3} \left(\frac{r}{a}\right)^3 \Delta U_0 + 4\pi \left(\frac{r}{a}\right)^2 g \\ &= -\frac{4\pi r^3}{3a^3} \Delta U_0 + 4\pi r^2 \alpha, \end{aligned} \quad (12)$$

where $\alpha = \frac{g}{a^2}$.

The Physical meaning of this result follows from the presentation in terms of radial force,

$$\begin{aligned} f &= -\frac{\partial U}{\partial r} = -\frac{\partial}{\partial r} \left(-\frac{4\pi r^3}{3a^3} \Delta U_0 + 4\pi r^2 \alpha \right) \\ &= 4\pi r^2 \frac{\Delta U_0}{a^3} - 8\pi r \alpha. \end{aligned} \quad (13)$$

The first, positive term describes the internal “pressure” in the radial direction tending to enlarge the PNR,

$$P = \frac{\text{Radial force}}{\text{Surface area of the sphere}} = \frac{4\pi r^2 (\Delta U_0 / a^3)}{4\pi r^2} = \frac{\Delta U_0}{a^3}. \quad (14)$$

It reflects the tendency to gain internal energy PV with $V = (4/3)\pi r^3$ by increasing the number of ordered dipoles. Noteworthy, the pressure $P = \Delta U_0 / a^3 = \text{const.}$ is size independent. Hence, growth of the PNR is an “isobaric” process. The second term, originating from the surface layer, is negative; it compresses the sphere, quite similar to “surface tension.” Neither “pressure” nor “surface tension” used here has anything to do with real pressure and surface tension in actual gases, liquids, and/or other macroscopic interfaces. The terms “pressure” and “surface tension” (in quotation marks!) are introduced here for the sake of simplicity, appealing to and providing for a formal analogy with the well-known formulas of surface tension in physics of condensed matter [33]. The algebraic similarity is the only reason for introducing the constant $\alpha = g/a^2$. In our case it plays the role of the coefficient of “surface tension.” As follows from (12) and (13), the additional “pressure” created by the “surface tension,” is

$$\Delta P_{\text{st}} \approx -\frac{8\pi R\alpha}{4\pi r^2} = -\frac{2\alpha}{r}. \quad (15)$$

Notably, the negative sign in Eq. (15) means that it acts as an “external” force, and the last term in Eq. (13) describes the work, $W = 4\pi R^2 \alpha$, performed on the PNR by the force of “surface tension.”

For the system in a thermostat under consideration, exchange of energy with the environment may take place without free energy conservation, $\Phi_i \neq \Phi_f$, the total energy balance being preserved by compensation of the heat transfer, $Q = T(S_f - S_i) = T\Delta S$, with internal energy change ΔU and mechanical work of internal forces, W_{intern} . Similar to other processes with heat (entropy) transfer, formation of PNRs is a nonequilibrium thermodynamic process, described by Gibbs free energy change, $\Delta G = \Delta H - T\Delta S$, where ΔH is the change of enthalpy H . With the growing size of the PNRs, their Gibbs free energy decreases and reaches a minimum value when n satisfies the condition of thermodynamic equilibrium with the environment, at which point the shape-restoring force, $-dG/dr$, is close to zero, while according to the first law of thermodynamics, $\Delta U = Q - W_{\text{intern}}$. In our case, in the process of the n -center PNR formation the system changes from the initial cubic disordered phase to the final partially ordered tetragonal one, for which $Q = T(S_f - S_i) = T_n(S_n^{(\text{tetr})} - S_n^{(\text{cub})})$, $\Delta U = U_f - U_i = U_n^{(\text{tetr})} - U_n^{(\text{cub})} = n\Delta U_0$, and $W_{\text{intern}} = 4\pi r^2 \alpha \approx 4.8gn^{2/3}$. Note that the work of internal forces is positive, $W_{\text{intern}} > 0$, whereas the heat transfer is negative, $Q < 0$, meaning heat is transferred to the environment. Accordingly,

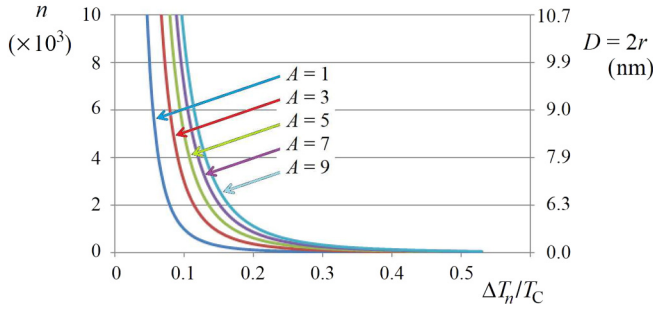


FIG. 8. Temperature dependence of the PNR size shown by the number of centers n ($\times 10^3$, left scale), and the diameter of its spherical form D (in nm, right-side scale), as a function of the crystal parameter A .

the first law of thermodynamics in this case acquires the following form:

$$T_n(S_n^{(\text{cub})} - S_n^{(\text{tetr})}) = n\Delta U_0 + W_{\text{intern}} = n\Delta U_0 + 4.8gn^{2/3}. \quad (16)$$

Introduced above in Eq. (7), $g = U_{\text{tet}}^{(\text{surf})} - U_{\text{tet}}^{(\text{in})}$ is the energy disadvantage (per one unit cell) of the dipoles on the surface of the PNR compared with the ones inside it. Using the equation of the macroscopic phase transition at the Curie temperature, $T_C(S_0^{(\text{cub})} - S_0^{(\text{tetr})}) = \Delta U_0$, and substituting $S_n^{(\text{cub})} = nS_0^{(\text{cub})}$ and $S_n^{(\text{tetr})} = nS_0^{(\text{tetr})}$, we get the relation between the temperature increment $\Delta T_n = T_n - T_C$ and the size n of the PNR, illustrated in Fig. 8:

$$\Delta T_n = T_C \frac{4.8g}{\Delta U_0} n^{-1/3}, \quad (17)$$

or, equivalently,

$$\frac{T_n}{T_C} = 1 + \frac{4.8g}{\Delta U_0} n^{-1/3}, \quad T_n = T_C \left(1 + \frac{4.8g}{\Delta U_0} n^{-1/3} \right).$$

IV. DISCUSSION OF THE RESULTS: NUMERIC ESTIMATES

Referring to formation of the PNR that follows from the above treatment of the problem, we see that the growth of the spherical PNR is subject to the larger “pressure” from inside the sphere, tending to align the local dipolar displacements, as compared with the compressing force of the “surface tension.” It follows from Eq. (13) that the force of the inner pressure is proportional to r^2 (to the border surface area $4\pi r^2$), whereas the compressing force $4\pi r\alpha$ is proportional to r . This means that, since $r > a$ and $n = \frac{4\pi}{3} \left(\frac{r}{a}\right)^3$, at $n \geq 4$ the force increasing the PNR size is dominant. Although the thermodynamic considerations employed in the treatment of this process are not applicable to very small numbers of centers, this conclusion shows the tendency in a qualitative manner. It means that in the fully disordered paraelectric phase, any small fluctuation that aligns the averaged dipole moments of —three to four centers [their mean field; see Fig. 4(a)] triggers further ordering, causing the growth of the PNR. Like in a process of self-assembly, the local ordering continues until the energy gain due to the progressive loss of entropy, $(-T\Delta S)$, is

exhausted by covering the loss in potential energy $n\Delta U_0$ and the work against the compressing effect of “surface tension.”

The entropy part is transferred to the environment (dissipated) in the form of heat, $Q_n = T\Delta S_n$. Obviously, this process cannot be reversed: the probability of a heat (or entropy) transfer from the bulk back to the given PNR is negligible. This provides stability to the PNR in the disordered environment. Once grown to its equilibrium size (to the minimum of the above-noted Gibbs free energy), the PNR cannot be destroyed by thermal fluctuations unless the temperature is increased or an external electric field is applied [34]. These estimates show also that an initial trigger (fluctuation), albeit small, is needed to start the growth of a PNR. It explains the role of crystal imperfections or structural irregularities (particularly, in mixed perovskites) in the formation of a PNR.

From Eq. (17) we get the temperature dependence of the number of centers in the thermodynamically equilibrated PNR:

$$n = A \left(\frac{T_n}{T_C} - 1 \right)^{-3} = \frac{A}{(\Delta T/T_C)^3}, \quad (18)$$

where $A = 36\pi \left(\frac{g}{\Delta U_0}\right)^3$ is a crystal parameter. With the dependence of the number of centers n on the radius r of the spherical PNR [Eq. (9)], we obtain also its diameter D as a function of temperature,

$$D = 2r \approx 1.24a\sqrt[3]{A} \left(\frac{T_n}{T_C} - 1 \right)^{-1} = \frac{1.24a\sqrt[3]{A}}{\Delta T/T_C}. \quad (19)$$

With regard to the crystal parameter A , the above estimate $g \approx \frac{1}{6}\Delta U_0$ [see Fig. 5 and the text before Eq. (7)] is based on the assumption that the PNR surface wall is planar, meaning $r \rightarrow \infty$, and only one lattice-constant layer is affected by the reduced-to-zero mean field of the outside fully disordered cubic phase. In fact, PNRs are small with small r values, and for rounded walls the restraining contribution of the outside centers is significantly larger, meaning the mean field in the surface layer is much weaker. In addition, the outside zero mean field may reduce the effective mean field and tetragonal ordering in more than one lattice layer, thus significantly increasing the g value. Since $A \sim g^3$, a reasonable estimate yields $1 < A < 10$.

For instance, for BaTiO_3 , $T_C = 360$ K, $T_B \approx 600$ K, and for $A = 5$, we get $n \approx 17$ at the Burns temperature, which for a spherical PNR means $D = 2r \approx 1.3$ nm, while for $A = 10$, $n \approx 34$ and $D \approx 1.7$ nm. This is the size of the PNR, which is assumed to become undetectable in BaTiO_3 at the Burns temperature. On the other hand, the dependence of the PNR size on temperature is much stronger. For instance, for BaTiO_3 at $T \sim 400$ K, $\Delta T/T_C \approx 0.1$, and at $A = 5$, $n \sim 10^3$ – 10^4 and $D \sim 9$ nm (at $A = 10$, $D \sim 11$ nm). Roughly, the PNR size in BaTiO_3 changes from ~ 1 nm at the Burns temperature to ~ 10 nm in the nonergodic state in the region near T_C . The temperature dependence of $n(T)$ and $D(T)$ for different values of the crystal parameter A are shown in Fig. 8.

Subject to the power “ -3 ” in Eq. (18) (see also Fig. 8), the increase of the size of the PNR with decrease of temperature is very fast, especially at smaller increments $\Delta T_n/T_C \approx 0.1$ – 0.2 . If, for instance, the temperature decreases linearly with time t , $T = T_{\text{init}} - mt$, where $T_{\text{init}} > T_C$, and $m = \text{const.} > 0$, then the

rate of PNR growth is

$$\frac{dn}{dt} = \frac{3mA}{T_C} \left(\frac{T}{T_C} - 1 \right)^{-4} = \frac{3AmT_C^3}{\Delta T^4}, \quad (20)$$

where $\Delta T = T - T_C$. For BaTiO₃ in the above conditions, $T_{\text{init}} \approx T_B \approx 600$ K and $A = 5$, even slow cooling with the rate $m = 0.1$ K/s yields a very fast increase of $(7 \times 10^7) \Delta T^{-4}$ centers per second. At the time when the temperature difference $\Delta T = T - T_C$ decreases to the order of 10 K, randomly polarized and arbitrarily located PNRs would cover the whole crystal sample, while their reorientation and ordering require much more time. As a result, at certain temperatures T_f , $T_C < T_f < T_B$, a nonergodic “glassy” polar phase occurs (like in dipolar glasses). It follows that two conditions are necessary for the occurrence of the nonergodic phase in relaxor ferroelectrics: (1) a high concentration of PNRs, and (2) relatively fast cooling. The first of these conditions is related also to structural inhomogeneity created by crystal imperfections and impurities; they favor the above-mentioned local fluctuations, which trigger the PNR formation. This explains why PNRs are best seen in mixed perovskite crystals. In sufficiently strong electric fields all the PNRs are repolarized in the same direction, so the glassy state disappears irreversibly, distinguished from polar glasses, but in full accordance with experimental data.

V. CONCLUSIONS

In this paper, relaxor properties of perovskite ferroelectrics and the nature of PNRs emerge from the first-principles microscopic theory of ferroelectricity, in which the spontaneous polarization of the crystal is triggered by the local dynamic-dipolar instability induced by the PJTE. In the framework of displacive approaches to the theory of ferroelectricity, which are based on the intrinsic assumption that only long-range interactions may produce the polarization, the formation of small (nanosize) polarized isles in the paraelectric phase is hardly possible. Created by lattice imperfections and irregularities, local inhomogeneity and “random fields” do lead to some local formations, but they are not temperature dependent, they do not grow when the crystal cools down below T_B , and do not disappear above T_B or under the influence of polarizing electric fields, and they cannot initiate formation of the “glassy” phase with cooling.

The occurrence of PNRs at $T > T_C$ in the disordered phase with dynamically oriented local dipolar displacements may be seen as an example of self-assembly. Centered somewhere about a crystal imperfection, it starts with a fluctuation in

the intercell dipolar alignments. If the newly created precursor exceeds the critical size of $n_{\text{crit}} \approx 3-5$, its spontaneous growth continues until the energy gain due to ordering is sufficient enough to cover both the progressive loss of entropy, $T\Delta S$, and the work against the compressing effect of “surface tension.” The spherical shape of PNRs with relatively large numbers of centers n follows from the condition of minimum “surface” energy (see also the spherical random-bond–random-field model [35], where the spherical shape was postulated), although at smaller n other shapes may be seen [36].

As a whole, the formation of the n -center PNR takes place in a nonequilibrium thermodynamic process, described by Gibbs free energy G , which reaches its minimum value at a certain size n , at which point $-dG/dr$ is close to zero. It means also that at this equilibrium size the amplitude of breathing vibrations of the PNR becomes noticeably big [37,38], which is seen in the low-frequency resonance dielectric spectra [39], and in the electro-optic effects [40].

We show that all the main properties of relaxor ferroelectrics follow directly from local polar dynamics induced by the PJT effect in the B center of the perovskite structure ABO_3 (A centers can be treated similarly): (i) With increasing temperature PNRs decrease in size, (ii) PNRs disappear above the Burns temperature and/or at any temperature in polarizing electric fields, and (iii) with fast cooling, it may lead to formation of the nonergodic “glassy” polar phase at $T = T_f$, approximately, at $(T_f - T_C)/T_C \sim 0.1-0.2$. Numerical estimates are obtained for BaTiO₃, for which the parameters of the PJT effect were estimated earlier in the vibronic (PJT) theory.

In many details (the trigger role of fluctuations, the role of internal “pressure,” the “surface tension,” etc.) the formation of PNRs, described in this paper, follows the *classical nucleation* theory [41–43]. However, there are also significant differences: Stable PNRs grow not in a metastable phase, but at temperatures well above T_C when the paraelectric phase is in thermodynamic equilibrium. This phenomenon is possible exclusively due to the PJTE: The off-center instability of the B ion results in its local polar displacements, which are randomly and relatively easy reorienting in the disordered cubic phase. In this respect, a ferroelectric perovskite crystal is akin to a polar liquid [44]. Accordingly, the “glassy state” is similar to a suddenly frozen polar liquid with its randomly oriented dipoles, but with an essential difference that the ferroelectric glassy state can be irreversibly eliminated in sufficiently strong electric fields.

-
- [1] A. A. Bokov and Z.-G. Ye, *J. Mater. Sci.* **41**, 31 (2006); *J. Adv. Dielectr.* **02**, 1241010 (2012); D. Wang, A. A. Bokov, Z.-G. Ye, J. Hlinka, and L. Bellaiche, *Nat. Commun.* **7**, 11014 (2016).
- [2] R. A. Cowley, S. N. Gvasaliya, S. G. Lushnikov, B. Roessli, and G. M. Rotaru, *Adv. Phys.* **60**, 229 (2011).
- [3] G. A. Samara, in *Solid State Physics, Advances in Research and Applications*, Vol. 56, edited by H. Ehrenreich and F. Spaepen (Academic, New York, 2001), p. 1; *J. Phys.: Condens. Matter* **15**, R367 (2003).
- [4] G. Xu, G. Shirane, J. R. D. Copley, and P. M. Gehring, *Phys. Rev. B* **69**, 064112 (2004).
- [5] G. Burns and F. H. Dacol, *Solid State Commun.* **48**, 853 (1983).
- [6] R. Fisch, *Phys. Rev. B* **67**, 094110 (2003).
- [7] E. V. Colla, P. Griffin, M. Delgado, M. B. Weissman, X. Long, and Z.-G. Ye, *Phys. Rev. B* **78**, 054103 (2008); M. Delgado, E. V. Colla, P. Griffin, M. B. Weissman, and D. Viehland, *ibid.* **79**, 140102(R) (2009).

- [8] W. Kleemann, J. Dec, and S. Miga, *Ferroelectrics* **499**, 72 (2016).
- [9] B. E. Vugmeister and M. D. Glinchuk, *Rev. Mod. Phys.* **62**, 993 (1990); B. E. Vugmeister, *Phys. Rev. B* **73**, 174117 (2006).
- [10] M. D. Glinchuk, A. V. Ragulya, and V. A. Stephanovich, *Nanoferroics*, Springer Series in Material Science, Vol. 177 (Springer Science + Business Media, Dordrecht, 2013), Chap. 3.
- [11] G. Geneste, *Phys. Rev. B* **79**, 064101 (2009); **79**, 144104 (2009).
- [12] H. Takenaka, I. Grinberg, S. Liu, and A. M. Rappe, *Nature* **546**, 391 (2017).
- [13] K. A. Müller and W. Berlinger, *Phys. Rev. B* **34**, 6130 (1986); K. A. Müller, W. Berlinger, K. W. Blazey, and J. Albers, *Solid State Commun.* **61**, 21 (1987); K. A. Müller and J. C. Fayet, in *Structural Phase Transitions II*, edited by K. A. Müller and H. Thomas (Springer-Verlag, Berlin, 1991), pp. 1–82; G. Völkel and K. A. Müller, *Phys. Rev. B* **76**, 094105 (2007).
- [14] R. Z. Tai, K. Namikawa, A. Sawada, M. Kishimoto, M. Tanaka, P. Lu, K. Nagashima, H. Maruyama, and M. Ando, *Phys. Rev. Lett.* **93**, 087601 (2004).
- [15] J.-H. Ko, S. Kojima, T.-Y. Koo, J. H. Jung, C. J. Won, and N. J. Hur, *Appl. Phys. Lett.* **93**, 102905 (2008); A. Ziębińska, D. Rytz, K. Szot, M. Górny, and K. Roleder, *J. Phys.: Condens. Matter* **20**, 142202 (2008); J.-H. Ko, T. H. Kim, K. Roleder, D. Rytz, and S. Kojima, *Phys. Rev. B* **84**, 094123 (2011).
- [16] M. A. Helal, M. Aftabuzzaman, S. Tsukada, and S. Kojima, *Sci. Rep.* **7**, 44448 (2017).
- [17] I. B. Bersuker, *Phys. Lett.* **20**, 589 (1966).
- [18] I. B. Bersuker, *Ferroelectrics* **536**, 1 (2018).
- [19] I. B. Bersuker, *Phys. Rev. Lett.* **108**, 137202 (2012).
- [20] V. Z. Polinger, P. Garcia-Fernandez, and I. B. Bersuker, *Phys. B (Amsterdam, Neth.)* **457**, 296 (2015).
- [21] V. Z. Polinger, *J. Phys.: Conf. Ser.* **428**, 012026 (2013).
- [22] I. B. Bersuker, *Appl. Phys. Lett.* **106**, 022903 (2015); **107**, 202904 (2015).
- [23] V. Z. Polinger and I. B. Bersuker, *J. Phys.: Conf. Ser.* **833**, 012012 (2017).
- [24] I. B. Bersuker, *J. Phys.: Conf. Ser.* **428**, 012028 (2013).
- [25] P. Zubko, G. Catalan, and A. K. Tagantsev, Flexoelectric effect in solids, *Annu. Rev. Mater. Res.* **43**, 387 (2013); A. Biancoli, C. M. Fancher, J. L. Jones, and D. Damjanovic, *Nat. Mater.* **14**, 224 (2015); A. N. Morozovska, V. V. Khist, M. D. Glinchuk, C. M. Scherbakov, M. V. Silibin, D. V. Karpinsky, and E. A. Eliseev, *J. Mol. Liquids* **267**, 550 (2018).
- [26] R. Comes, M. Lambert, and A. Guinier, *Solid State Commun.* **6**, 715 (1968).
- [27] B. Ravel, E. A. Stern, R. I. Vedrinskii, and V. Kraizman, *Ferroelectrics* **206–207**, 407 (1998); E. Stern, *Phys. Rev. Lett.* **93**, 037601 (2004).
- [28] B. Zalar, V. V. Laguta, and R. Blinc, *Phys. Rev. Lett.* **90**, 037601 (2003); B. Zalar, A. Lebar, J. Seliger, R. Blinc, V. V. Laguta, and M. Itoh, *Phys. Rev. B* **71**, 064107 (2005).
- [29] I.-K. Jeong, S. Lee, S.-Y. Jeong, C. J. Won, N. Hur, and A. Llobet, *Phys. Rev. B* **84**, 064125 (2011).
- [30] A. Pramanick, X. P. Wang, C. Hoffmann, S. O. Diallo, M. R. V. Jørgensen, and X.-L. Wang, *Phys. Rev. B* **92**, 174103 (2015).
- [31] A. K. Kalyani, D. K. Khatua, B. Loukya, R. Datta, A. N. Fitch, A. Senyshyn, and R. Ranjan, *Phys. Rev. B* **91**, 104104 (2015).
- [32] T. Egami, *Ferroelectrics* **235**, 101 (2002).
- [33] L. D. Landau and E. M. Lifshitz, *Statistical Physics, Course of Theoretical Physics*, Vol. 5 (Elsevier, Butterworth-Heinemann, 1980), Sec. 154.
- [34] K. Matsumoto and S. Kojima, *Jpn. J. Appl. Phys.* **54**, 10NC04 (2015).
- [35] R. Pirc and R. Blinc, *Phys. Rev. B* **60**, 13470 (1999).
- [36] G. Geneste, J.-M. Kiat, H. Yokota, Y. Uesu, and F. Porcher, *Phys. Rev. B* **81**, 144112 (2010); G. Yong, J. Toulouse, R. Erwin, S. M. Shapiro, and B. Hennion, *ibid.* **62**, 14736 (2000).
- [37] A. R. Bishop, A. Bussmann-Holder, S. Kamba, and M. Maglione, *Phys. Rev. B* **81**, 064106 (2010).
- [38] B. Cai, J. Schwarzkopf, E. Hollmann, D. Braun, M. Schmidbauer, T. Grellmann, and R. Wördenweber, *Phys. Rev. B* **93**, 224107 (2016).
- [39] S. Wakimoto, G. A. Samara, R. K. Grubbs, E. L. Venturini, L. A. Boatner, G. Xu, G. Shirane, and S. H. Lee, *Phys. Rev. B* **74**, 054101 (2006).
- [40] H. Tian, B. Yao, L. Wang, P. Tan, X. Meng, G. Shi, and Z. Zhou, *Sci. Rep.* **5**, 13751 (2015); P. Tan, H. Tian, Y. Wang, X. Meng, F. Huang, X. Cao, C. Hu, L. Li, and Z. Zhou, *Opt. Lett.* **43**, 5009 (2018).
- [41] J. Merikanto, E. Zapadinsky, H. Vehkamäki, and A. Lauri, *Phys. Rev. Lett.* **98**, 145702 (2007).
- [42] https://en.wikipedia.org/wiki/Classical_nucleation_theory, and references therein.
- [43] E. M. Lifshitz and L. P. Pitaevskii, *Physical Kinetics*, Course of Theoretical Physics, Vol. 10 (Butterworth-Heinemann, Oxford, 1981), Sec. 99.
- [44] Long before the discovery of ferroelectricity, this similarity was noticed by P. Debye, who suggested the possible existence of dielectric crystals with randomly oriented dipole moments (similar to ferromagnetics), which may behave like a polar liquid above its freezing point; P. Debye, *Phys. Z.* **13**, 97 (1912).